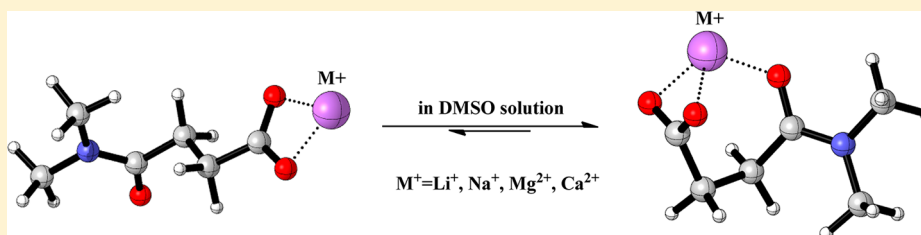


Conformational Preferences of *N,N*-Dimethylsuccinamate as a Function of Alkali and Alkaline Earth Metal Salts: Experimental Studies in DMSO and Water As Determined by ^1H NMR Spectroscopy

Holden W. H. Lai, Albert Tianxiang Liu, Bright U. Emenike, William R. Carroll, and John D. Roberts*

Gates and Crellin Laboratories of Chemistry, California Institute of Technology, Pasadena, California 91125, United States

S Supporting Information



ABSTRACT: The fraction of *gauche* conformers of *N,N*-dimethylsuccinamic acid (**1**) and its Li^+ , Na^+ , K^+ , Mg^{2+} , Ca^{2+} , and $\text{N}(\text{Bu})_4^+$ salts were estimated in DMSO and D_2O solution by comparing the experimental vicinal proton–proton couplings determined by ^1H NMR spectroscopy with those calculated using the Haasnoot, de Leeuw, and Altona (HLA) equation. In DMSO, the *gauche* preferences were found to increase with decreasing Ahrens ionic radius of the metal counterion. The same trend was not seen in D_2O , where the *gauche* fraction for all of the metallic salts were estimated to be approximately statistical or less. This highlights the importance of metal chelation on the conformation of organic molecules in polar aprotic media, which has implications for protein folding.

INTRODUCTION

Metal ions interactions are crucial for many biological processes including protein folding,¹ enzymatic catalysis,² and signal transduction.³ One of the important roles of metal cations in biological system is the maintenance of precise electrochemical gradients across cell membranes. Such electrochemical gradients have been studied extensively in essential biological mechanisms such as nutrients transport and the maintenance of resting and action potentials.^{4,5} However, many studies have also demonstrated that conformational changes caused by metal chelation can alter the biological activities of substances. For example, Mg^{2+} and Ca^{2+} can induce distinct and separate conformational changes in calcium-binding protein 1, increasing structural stability of the protein.⁶ In addition, the mechanism involved in muscle contraction is initiated by the complexation of Ca^{2+} to calmodulin that is activated by concomitant conformational changes. Also, the binding of Mg^{2+} to three aspartic acid residues in CheY, a signal transduction protein in bacteria, facilitates activation of the protein.⁷

Investigation of metal-induced conformational changes at the molecular level within biological systems is often complicated by other competing forces such as hydrogen bonds. Therefore, it is much more convenient to study simpler model systems, where a specific interaction of interest can be isolated. For example, Juaristi et al. used a 5-acetoamido-1,3-dioxane derivative to show that LiBr is capable of disrupting intramolecular amide hydrogen bonds through the formation of a six-membered ring LiBr complex.⁸ A subsequent extension

of Juaristi's study using 5-carboxy-1,3-dioxanes revealed an increase in the stability of the axial isomer with Ag^+ and Li^+ salts, while larger metal ions such as Na^+ and K^+ had only marginal effects.⁹ In a recent paper, Roberts et al. examined the conformational preferences of *N,N*-dimethylsuccinamic acid (**1**, DMSA), its tetrabutylammonium salt (**1e**), and its lithium salt (**1a**). Interestingly, **1a** resulted in an overwhelming preference for the *gauche* conformer (Figure 1) in aprotic solvents, while **1e** remained predominantly *trans* (anti).¹⁰ The un-ionized **1**

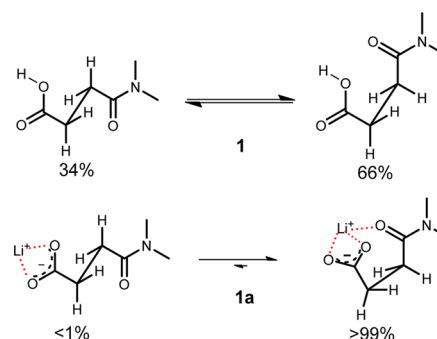


Figure 1. Conformational equilibria of *N,N*-dimethylsuccinamic acid (**1**, top) and its lithium salt (**1a**, bottom) in DMSO.

Received: October 28, 2013

Revised: February 4, 2014

Published: February 7, 2014

was determined to have a statistical *gauche* fraction of 0.66, indicating no preference for either the *gauche* or *trans* conformers. The conformational equilibrium of **1a** were found to be strongly solvent-dependent, such that the solvents' hydrogen bonding strength as measured by Kamlet–Taft's α scale was a dominant factor.¹⁰

In this paper, the conformational study of **1** has been extended by including the Na⁺, K⁺, Mg²⁺, and Ca²⁺ salts. *N,N*-Dimethylsuccinamic acid (**1**) is particularly suitable for mimicking metal chelation in biological systems because both the carboxylate and amide metal complexes are commonly found in polypeptides.¹¹ The motivation behind this work is to draw parallels between the conformational preferences of **1** as a function of these salts in DMSO and water as solvents. While water as a solvent imitates the aqueous environments commonly found in biological systems, DMSO mimics the polar aprotic media found in the interior of folded polypeptides.

RESULTS AND DISCUSSIONS

Model System. Simple 1,2-disubstituted ethane systems such as *N,N*-dimethylsuccinamic acid (**1**) are efficient models to study intramolecular interactions because they adopt well resolved *gauche* and *trans* conformers (Figure 2), where

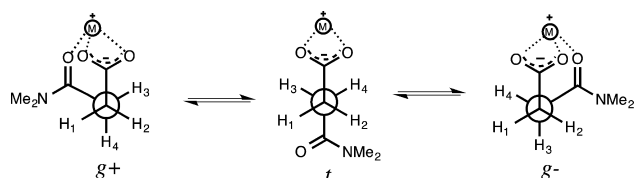


Figure 2. Two possible *gauche* (*g+* and *g-*) and *trans* (*t*) conformers of *N,N*-dimethylsuccinamate, where M⁺ represents the alkali ions (Li⁺, Na⁺, and K⁺) and alkaline earth ions (Mg²⁺ and Ca²⁺). The various geometries were deduced from computational modeling (*vide infra*) in the gas phase.

intramolecular noncovalent interactions can stabilize the *gauche* conformations. Because there are two possible *gauche* and one *trans* staggered conformers, the preference for each conformer can be deduced by measuring the ratios of their respective populations using proton (¹H) NMR spectroscopy. In the absence of any preferential stabilization, the statistical *gauche* fraction (*F_g*) should be 0.67. Therefore, an *F_g* value greater than 0.67 indicates stabilization of the *gauche* conformer, plausibly by intramolecular interaction. On the other hand, *F_g* values less than 0.67 suggest an antagonistic relationship between the two substituents on the ethane, which may be due to electrostatic and/or steric repulsions.

The *gauche* fraction of each conformer was estimated by comparing the experimental vicinal proton coupling constants (³*J_{HH}*) measured by ¹H NMR spectroscopy with their semiempirical counterparts calculated using the Haasnoot, de Leeuw and Altona (HLA) equation (eq 2).¹² Equation 2 is an improved version of the original equation.¹³ Because the rotation about the “CH₂–CH₂” bond is rapid at room temperature, the experimental vicinal coupling constants (³*J_{obs}*) represent weighted averages of the individual couplings for the *gauche* and *trans* conformers, as described by eq 1. Note here that sum of the fractions is unity, i.e., *F_g* + *F_t* = 1. Also note that two experimental ³*J_{obs}* values, i.e., ³*J₁₃* and ³*J₁₄* (where ³*J₁₃* = ³*J₂₄* and ³*J₁₄* = ³*J₂₃*) can be used to provide independent values for *F_g* and *F_t*.

$$^3J_{\text{HH(obs)}} = \sum F_j J_j = (^3J_{\text{HH(g)}} \times F_g) + (^3J_{\text{HH(t)}} \times F_t) \quad (1)$$

$$^3J_{\text{HH(semiempirical)}} = 14.63 \cos^2 \varphi_{ij} - 0.78 \cos \varphi_{ij} + 0.60 + \sum \lambda_i [0.34 - 2.31 \cos^2(\zeta_i \varphi_{ij} + 18.4|\varphi_i|)] \quad (2)$$

The HLA equation gives more accurate results than the traditional Karplus equation because it takes into account the orientation and electronegativity variables (λ) of the substituent groups attached to the central C–C fragment. The electronegativity values for CO₂[−], CO₂H, and CONMe₂ have been reported elsewhere.¹⁴ The parameter ζ_i can take the values +1 or −1 depending on the relative orientation of the substituents. The essential dihedral angles (φ) were derived from geometries of the optimized structures from DFT calculations.

Computational Analysis. Conformational searches for Na⁺(**1b**), K⁺(**1c**), Ca²⁺(**1d**), and Mg²⁺(**1e**) salts of *N,N*-dimethylsuccinamic acid were first performed with SPARTAN at the molecular mechanics level. These preliminary calculations provided guess-structures for subsequent DFT calculations. The DFT calculations were carried out at the B3LYP/6-31+G(2d,2p) level in the gas phase using Gaussian 03 program.¹⁵ Subsequent free energy calculations at the same level as the optimized structures determined the relative free energies and revealed that the gas phase optimized structures were of stable forms and not transition states.¹⁵

The graphical representations of the DFT gas phase optimized structures are shown in Figure 3. Distances of carboxylate-metal ion complex in the respective *gauche* conformers for **1a**–**1c** were calculated to be greater than their *trans* counterparts in each case. For example, the

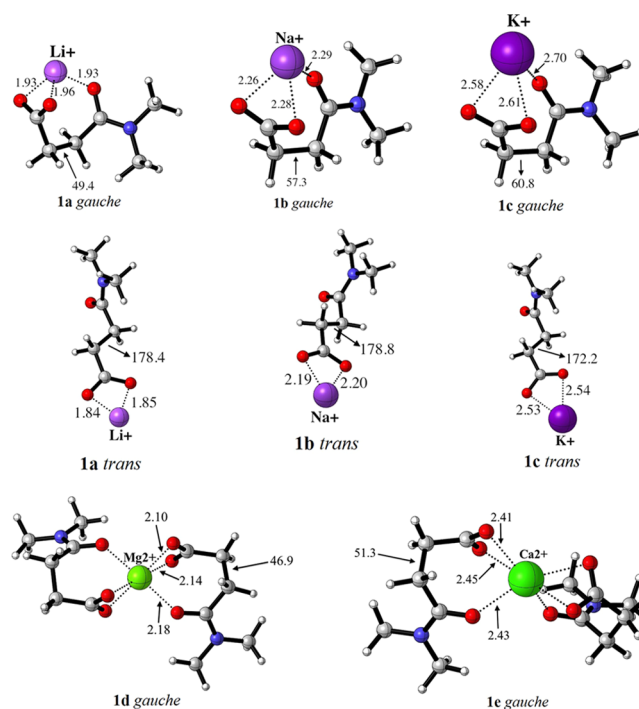


Figure 3. DFT-optimized structures for the *gauche* (top) and *trans* (middle) conformers of **1a**–**1c** and *gauche* (bottom) conformers of **1d**–**1e** at the B3LYP/6-31+G(2d,2p) level of theory in the gas phase. The calculated metal–oxygen distances are in Å, and the shown dihedral angles are in deg. Ahrens ionic radii were used to illustrate the metal ions.

calculated Li⁺–O distances for **1a** (1.93–1.96 Å) in the *gauche* conformer are consistent with the values of 1.90–2.67 Å found in lithium-carboxylate X-ray crystal structures,^{16–18} while the values of 1.84–1.85 Å observed in the *trans* conformer appear to be slightly underestimated. The calculated Na⁺–O distances (2.26–2.29 Å) in *gauche* **1b** and the K⁺–O distance in *gauche* **1c** (2.58–2.70 Å) matched the values observed in crystal structures (i.e., 2.26–2.67 Å and 2.36–2.73 Å, respectively),^{19–22} whereas the values in the *trans* conformers are slightly lower (i.e., 2.19–2.20 Å for **1b** and 2.53–2.54 Å for **1c**). As for the divalent metal salts, the calculated Ca²⁺–O distances (2.41–2.45 Å) in **1d** are within range of values found in crystal structures (2.26–2.59 Å).²³ The calculated Mg²⁺–O distances (2.10–2.18 Å) however, are slightly greater than the values found in crystal structures (1.99–2.09 Å),^{24,25} which could be a result of differential packing forces in the solid state.

Interestingly, the calculated lowest-energy *gauche* conformers for **1b** and **1c** were similar to that previously calculated for the lithium salt (**1a**)¹⁰ in the sense that the metal ions preferred to bridge the carboxylate and amide oxygen atoms (Figure 3). For **1a–1c**, DFT calculations in the gas phase estimated that these *gauche* conformers are more stable than their *trans* counterparts for every case. The calculated free energy of the *gauche* conformer of **1a** is 3.8 kcal/mol more stable than the *trans* conformer. On the other hand, the *gauche* conformer of the sodium salt (**1b**) was calculated to be only 1.4 kcal/mol more stable than the *trans* conformer, while the calculated *gauche*/*trans* energy difference is 1.6 kcal/mol for the potassium salt (**1b**). Free energies of all the DFT gas phase optimized structures can be found in the Supporting Information.

Efforts were also made to investigate the possibility of an alternative *gauche* geometry, that is, where only one of the carboxylate oxygen atoms coordinates to the metal ions. However, the calculations produced *gauche* conformers of relatively higher energy than previously calculated. Other conformational possibilities for **1a–1c** may involve aggregation, particularly for **1a**. Lithium salts are known to form dimers, tetramers and higher-order aggregates.²⁶ However, molecular mechanics calculations showed that, even in such aggregates (dimer and tetramer, for example), both the *gauche* and *trans* conformers can still exist. The differences in the *gauche* structures calculated for the monovalent metal salts (**1a–1c**) were, however, noticeable in the calculated dihedral angles. For example, of the three alkali metal salts, **1a** had the smallest φ_g value of 49.4°, and **1c** had the largest value of 60.8°. It is reasonable to suggest that as the Ahrens ionic radius^{27,28} of the metal counterion increases, the dihedral angle widens in order to snugly accommodate the metal ions. Note that these angles are smaller than the value of 76.7° calculated for the un-ionized **1**, where “weak” hydrogen bond has been suggested as the only stabilizing mechanism for the *gauche* conformer.¹⁰

Unlike **1a–1c**, the DFT gas phase optimized structure of divalent alkaline earth metal salts (**1d–1e**) share a single metal cation between two molecules of *N,N*-dimethylsuccinamate. The divalent metal cation coordinates to six oxygen atoms, forming a very distorted octahedral geometry, as shown in Figure 3. A randomized conformational search by molecular mechanics calculations for the divalent metal salts did not find any conformers in which *N,N*-dimethylsuccinamate adopted the *trans* conformation, which is not surprising considering the higher valency of Mg²⁺ and Ca²⁺ as well as their stronger chelation to the amide relative to the alkali metals.²⁹ Synonymous to the trend observed for the alkali metal salts,

φ_g also increases with increasing Ahrens ionic radii for **1d** and **1e**, where **1d** has a smaller calculated φ_g of 46.9° and φ_g 51.3° for **1e**.

The calculated dihedral angles were used to estimate *gauche* fractions of **1a–1e** in DMSO solution. In aqueous solvents, however, one would expect that both the carboxylate and metal cation would be strongly solvated by water molecules, which should result in the complete dissociation of the ion pairs. Because hydrated metal ions have larger ionic radii,³⁰ it is reasonable to assume that the actual φ_g in aqueous solution should be greater than the calculated angles for **1a–1e**. Furthermore, explicit solvent–solute hydrogen bond interactions in D₂O are often poorly captured by the current continuum solvation model (such as the IEFPCM and CPCM) employed by DFT calculations in the gas phase. For practical purposes, the φ_g for measurements in aqueous solution was assumed to be 60° while the *trans* angle to be 180°.

Experimental ³J_{HH} Coupling Constants. With the calculated dihedral angles in hand, the next task is to determine the J_{ij} experimental ³J_{HH} coupling constants. NMR simulation software (gNMR 5.0)³¹ was used to iteratively reproduce the experimental ¹H NMR spectra of the methylene protons region. Such simulations are essential because they provide an accurate depiction of the “real” coupling constants using 4-spin, AA'XX' systems. The chemical shifts for the methylene protons are different for all the salts prepared, however, their spin–spin splitting appeared as doublet of triplets (Figure 4).

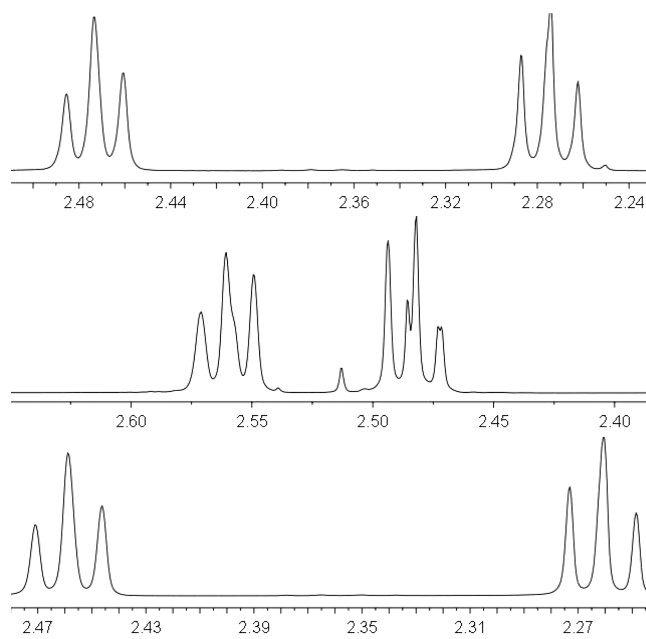


Figure 4. Stacked spectra of DMSA (**1**, top), its tetrabutylammonium salt (**1f**, middle), and its lithium salt (**1a**, bottom) in D₂O, spectral unit recorded in ppm.

Conformational Analysis. Using the vicinal proton–proton coupling constants obtained from simulation of the experimental ¹H NMR spectra and the dihedral angles from DFT gas phase calculations, the respective F_g values for **1a–e** were estimated as discussed earlier (Table 1 and 2). Compared to the un-ionized **1**, which has a small *gauche* fraction of 0.66 ± 0.01 ,¹⁰ the metal salts generally showed higher *gauche* fraction in DMSO. The relatively small *gauche* fraction estimated for **1** in DMSO is likely the result of the carboxylic acid’s unfavorable

Table 1. Experimental Vicinal H–H Couplings for the *N,N*-Dimethylsuccinamic Acid Salts (1a–1e) in DMSO and D₂O, Measured in Units of Hz

solvents	Li ⁺ salt 1a ^a		Na ⁺ salt 1b		K ⁺ salt 1c		Mg ²⁺ salt 1d		Ca ²⁺ salt 1e	
	<i>J</i> ₁₃	<i>J</i> ₁₄	<i>J</i> ₁₃	<i>J</i> ₁₄	<i>J</i> ₁₃	<i>J</i> ₁₄	<i>J</i> ₁₃	<i>J</i> ₁₄	<i>J</i> ₁₃	<i>J</i> ₁₄
DMSO	6.02	8.13	6.64	7.75	6.64	8.36	6.08	8.18	7.29	7.31
D ₂ O	6.59	8.33	7.08	7.35	7.04	7.94	7.28	7.31	6.36	8.37

^aData obtained from ref 10.**Table 2.** Estimated Fraction *Gauche* (*F_g*) for the *N,N*-Dimethylsuccinamic Acid Salts (1a–1e) and the Ahrens Ionic Radii^c (in Å) of the Metal Counter Ions^a

solvent	gauche fractions (<i>F_g</i>)				
	Li ⁺ salt 1a ^b	Na ⁺ salt 1b	K ⁺ salt 1c	Mg ²⁺ salt 1d ^d	Ca ²⁺ salt 1e
DMSO	1.00 ± 0.03	0.78 ± 0.02	0.55 ± 0.01	0.99 ± 0.04	0.79 ± 0.01
D ₂ O	0.55 ± 0.02	0.68 ± 0.01	0.61 ± 0.01	0.67 ± 0.01	0.53 ± 0.05
radii (Å) ^c	0.68	0.97	1.33	0.66	0.99

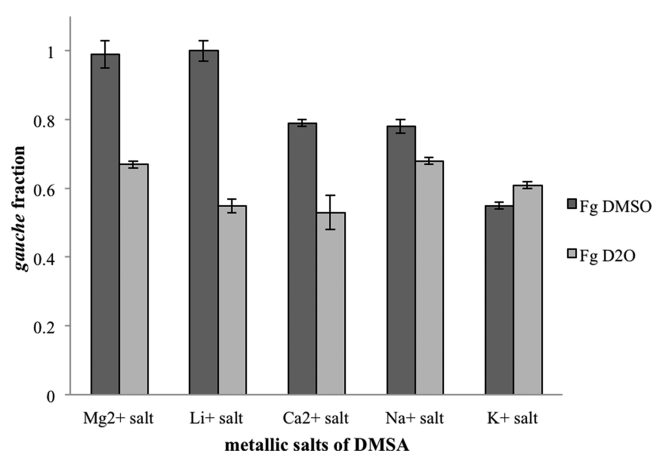
^aThe error in *F_g* is the deviation of using the *J*₁₃ and *J*₁₄ coupling constants for calculations. ^bData obtained from ref 10. ^cAhrens ionic radii were obtained from ref 28. ^d*F_g* in DMSO was obtained assuming the dihedral angle to be 50°.

E configuration (Figure 5) that must be adopted in order to form an intramolecular hydrogen bond.³²

**Figure 5.** *E* and *Z* configurations of a carboxylic acid. Also see Figure 1

In DMSO, the changing influence of the metal cation on the conformational preferences of *N,N*-dimethylsuccinamate is evident from the experimentally estimated *gauche* fractions of 1a–1e. Of the alkali metal salts, both the lithium and sodium salts (1a and 1b, respectively) showed preferences for the *gauche* conformer. 1a has the higher *gauche* fraction of 1.00, followed by 0.78 for 1b. These estimated *gauche* preferences are in agreement with DFT gas phase calculations, which predicted the *gauche* conformer to be more stable in both cases. DFT gas phase calculations also estimated the energy difference between the *gauche* and *trans* conformer of the lithium salt to be the highest among all the alkali metal salts, hence 1a's relatively high *gauche* preference. The potassium salt (1c) on the other hand, has a much lower *gauche* fraction of 0.55 in DMSO, which suggests that 1c prefers the *trans* conformer. As for the alkaline earth metal ions, both the magnesium and calcium salts (1d and 1e, respectively) have relatively high preferences for the *gauche* conformer in DMSO. For 1d, when the DFT calculated φ_g of 46.9° was used for the estimation of the *gauche* fraction, a value of 1.07 ± 0.05 was obtained. This is likely due to the underestimation of φ_g by DFT gas phase calculations, as adjusting the φ_g to 50° yielded a *gauche* fraction of 0.99 ± 0.04 .

The calculated *gauche* fractions for the metal salts (1a–1e) are shown schematically in Figure 6 as a function of the Ahrens ionic radius of the metal counterion. For the metal salts in DMSO, it is apparent that *gauche* fractions of the salts decrease with increasing Ahrens ionic radii of the metal counterion. Metal cations with smaller Ahrens ionic radii are likely able to better fit between the amide oxygen atom and carboxylate to bridge the two functional groups and induce *gauche* preference in *N,N*-dimethylsuccinamate. This assertion is supported by the DFT calculation results shown in Figure 3, where metal

**Figure 6.** Trend in conformational equilibria of the metallic salts of *N,N*-dimethylsuccinamic acid as a function of its cationic counterion, arranged from left to right in decreasing Ahrens ionic radius of the metal counterion.

counterions with smaller Ahrens ionic radii resulted in shorter metal–oxygen distances and smaller dihedral angles. In the case of 1c, K⁺ is likely too large to allow a proper fit between the amide and carboxylate.

In D₂O however, the interaction between *N,N*-dimethylsuccinamate and metal cations appears significantly different. No noticeable correlation between the Ahrens ionic radius of the metal counterion and *gauche* fraction of the *N,N*-dimethylsuccinamate could be established. For the metallic salts in D₂O, there is generally a lower *gauche* preference than in DMSO. In fact, none of the *N,N*-dimethylsuccinamate salts investigated have *gauche* fractions significantly higher than the statistical value of 0.67. The lack of *gauche* preferences in aqueous solution can be explained by the solvation efficiency of water. Water molecules can isolate and solvate cations (metal cation) and anions (carboxylates) appreciably well. Such isolated solvation would greatly diminish interactions between metal ions and *N,N*-dimethylsuccinamate. Previous study also found that 1a has a lower *gauche* fraction in solvents with better hydrogen donor propensities, which are also solvents likely to solvate anions efficiently.¹⁰

CONCLUSIONS

Using ^1H NMR spectroscopy, we have demonstrated that the conformational equilibria of DMSA and its metal salts are strongly solvent dependent. In DMSO solution, as the Ahrens ionic radius of the metal counterion increases, the *gauche* fraction of *N,N*-dimethylsuccinamate decreases. Interestingly, DFT calculations strongly suggest that the *gauche* preferences of the metallic salts are caused by cationic bridging of the amide and carboxylate oxygen atoms. The same interaction is much weaker in D_2O , where the estimated *gauche* fractions were significantly below the statistical 0.67 value. These results seem to suggest that metal chelation has an especially powerful influence on the conformation of organic molecules in polar aprotic media.

EXPERIMENTAL SECTION

Commercial *N,N*-dimethylsuccinamic acid (**1**) of ~98% purity was used without further purification. The $\text{Na}^+(\textbf{1b})$ salt was prepared by treating **1** with an equivalent mole of NaH in THF. The $\text{K}^+(\textbf{1c})$ salt was prepared by treating **1** with an equivalent mole of KCN. The $\text{Mg}^{2+}(\textbf{1d})$ and $\text{Ca}^{2+}(\textbf{1e})$ salts were prepared by treating **1** with 0.5 equiv of $\text{Mg}(\text{OH})_2$ and $\text{Ca}(\text{OH})_2$ respectively in water. Solvent was then evaporated and samples were dried *in vacuo*. Commercial $\text{DMSO}-d_6$ and D_2O were used without further purifications.

The ^1H NMR spectra were taken with Varian 300, 400, and 600 MHz spectrometers at 25 °C. See Supporting Information for specific acquisition parameters of each sample.

ASSOCIATED CONTENT

Supporting Information

Experimental ^1H NMR spectra and Cartesian coordinates of the optimized structures from DFT calculations. This material is available free of charge via the Internet at <http://pubs.acs.org>.

AUTHOR INFORMATION

Corresponding Author

*(J.D.R.) E-mail: robertsj@caltech.edu. Telephone: 626-395-6036.

Notes

The authors declare no competing financial interest.

ACKNOWLEDGMENTS

Acknowledgement is made to the National Science Foundation under Grant CHE-0543620, TG-CHE1000106, and to the donors of the Petroleum Research Fund, administered by the American Chemical Society, for support for this research. Other important support came from the Summer Undergraduate Research Fellowship Program (SURF) at the California Institute of Technology, the Amgen Foundation, the Senior Scientist Mentor Program of the Camille and Henry Dreyfus Foundation, and the Chemistry NORAC grant of Dr. and Mrs. Chester M. McCloskey. We are also indebted to Merck and Company, Dr. David J. Mathre, and Edith M. Roberts for their helpful financial assistance. The facilities of the MCS used in these studies were established with grants from DURIP-ONR and DURIP-ARO, with additional support from ONR, ARO, NSF, NIH, DOW, Chevron Nissan, Dow Corning, Intel, Pfizer, Boehringer-Ingelheim, and Sanofi-Aventis.

REFERENCES

- (1) Rigby Duncan, K. E.; Stillman, M. J. Metal-Dependent Protein Folding: Metallation of Metallothionein. *J. Inorg. Biochem.* **2006**, *100*, 2101–2107.
- (2) Andreini, C.; Bertini, I.; Cavallaro, G.; Holliday, G.; Thornton, J. Metal Ions in Biological Catalysis: from Enzyme Databases to General Principles. *J. Biol. Inorg. Chem.* **2008**, *13*, 1205–1218.
- (3) Zhou, L.; Li, S.; Su, Y.; Yi, X.; Zheng, A.; Deng, F. Interaction between Histidine and Zn(II) Metal Ions over a Wide pH as Revealed by Solid-State NMR Spectroscopy and DFT Calculations. *J. Phys. Chem. B* **2013**, *117*, 8954–8965.
- (4) Johansson, M.; Karlsson, L.; Wennergren, M.; Jansson, T.; Powell, T. L. Activity and Protein Expression of Na^+/K^+ ATPase Are Reduced in Microvillous Syncytiotrophoblast Plasma Membranes Isolated from Pregnancies Complicated by Intrauterine Growth Restriction. *J. Clin. Endocrinol. Metab.* **2003**, *88*, 2831–2837.
- (5) Orlov, S. N.; Hamet, P. Intracellular Monovalent Ions as Second Messengers. *J. Membr. Biol.* **2006**, *210*, 161–172.
- (6) Wingard, J. N.; Chan, J.; Bosanac, I.; Haeseleer, F.; Palczewski, K.; Ikura, M.; Ames, J. B. Structural Analysis of Mg^{2+} and Ca^{2+} Binding to CaBP1, a Neuron-specific Regulator of Calcium Channels. *J. Biol. Chem.* **2005**, *280*, 37461–37470.
- (7) Solà, M.; López-Hernández, E.; Cronet, P.; Lacroix, E.; Serrano, L.; Coll, M.; Parraga, A. Towards Understanding a Molecular Switch Mechanism: Thermodynamic and Crystallographic Studies of the Signal Transduction Protein CheY. *J. Mol. Biol.* **2000**, *303*, 213–225.
- (8) Juaristi, E.; Díaz, F.; Cuéllar, G.; Jiménez-Vázquez, H. A. Conformational Analysis of 5-Substituted 1,3-Dioxanes. 7. Effect of Lithium Bromide Addition. *J. Org. Chem.* **1997**, *62*, 4029–4035.
- (9) Vázquez-Hernández, M.; Rosquete-Pina, G. A.; Juaristi, E. Salt Effects on the Conformational Behavior of 5-Carboxy- and 5-Hydroxy-1,3-dioxane. *J. Org. Chem.* **2004**, *69*, 9063–9072.
- (10) Liu, A. T.; Emenike, B. U.; Carroll, W. R.; Roberts, J. D. Conformational Equilibria of *N,N*-Dimethylsuccinamic Acid and Its Lithium Salt as a Function of Solvent. *Org. Lett.* **2013**, *15*, 760–763.
- (11) Wilson, C. J.; Apiyo, D.; Wittung-Stafshede, P. Role of Cofactors in Metalloprotein Folding. *Q. Rev. Biophys.* **2004**, *37*, 285–314.
- (12) Altona, C.; Francke, R.; Dehaan, R.; Ippel, J. H.; Daalmans, G. J.; Hoekzema, A.; Vanwijk, J. Empirical Group Electronegativities for Vicinal NMR Proton-Proton Couplings along a C-C Bond - Solvent Effects and Reparameterization of the Haasnoot Equation. *Magn. Reson. Chem.* **1994**, *32*, 670–678.
- (13) Haasnoot, C. A. G.; Deleeuw, F.; Altona, C. The Relationship between Proton-Proton NMR Coupling-Constants and Substituent Electronegativities 1. An Empirical Generalization of the Karplus Equation. *Tetrahedron* **1980**, *36*, 2783–2792.
- (14) Altona, C.; Ippel, J. H.; Hoekzema, A.; Erkelens, C.; Groesbeek, M.; Donders, L. A. Relationship between Proton-Proton NMR Coupling Constants and Substituent Electronegativities 5. Empirical Substituent Constants Deduced from Ethanes and Propanes. *Magn. Reson. Chem.* **1989**, *27*, 564–576.
- (15) Frisch, M. J.; Pople, J. A. *Gaussian 03*, Gaussian, Inc.: Wallingford, CT, 2004.
- (16) Banerjee, D.; Kim, S. J.; Li, W.; Wu, H.; Li, J.; Borkowski, L. A.; Philips, B. L.; Parise, J. B. Synthesis and Structural Characterization of a 3-D Lithium Based Metal–Organic Framework Showing Dynamic Structural Behavior. *Cryst. Growth Des.* **2010**, *10*, 2801–2805.
- (17) Fleck, M.; Schwendner, K.; Hensler, A. Two New Non-Centrosymmetric Lithium Salts of Glycine: Bis(glycine) Lithium Chromate Monohydrate and Bis(glycine) Lithium Molybdate. *Acta Crystallogr., Sect. C* **2006**, *62*, 122–125.
- (18) Wiesbrock, F.; Schmidbaur, H. The Structural Chemistry of Lithium, Sodium and Potassium Anthranilate Hydrates. *J. Chem. Soc., Dalton Trans.* **2002**, *24*, 4703–4708.
- (19) Zeng, H.; Li, T.; Yan, Z.; Luo, S.; Li, F. Two Porous Metal–Organic Frameworks Showing Different Behaviors to Sodium Cation. *Cryst. Growth Des.* **2010**, *10*, 475–478.
- (20) Fu, Y.; Su, J.; Zou, Z.; Yang, S.; Li, G.; Liao, F.; Lin, J. Syntheses, Structures, and Gas Adsorption Properties of Two Novel Cadmium–

Sodium Organic Frameworks with 1,3,5-Benzenetricarboxylate Ligands. *Cryst. Growth Des.* **2011**, *11*, 3529–3535.

(21) Karabach, Y. Y.; Kirillov, A. M.; da Silva, M. F. C. G.; Kopylovich, M. N.; Pombeiro, A. J. L. An Aqua-Soluble Copper(II)–Sodium Two-Dimensional Coordination Polymer with Intercalated Infinite Chains of Decameric Water Clusters. *Cryst. Growth Des.* **2006**, *6*, 2200–2203.

(22) Nagapradeep, N.; Sharma, S.; Verma, S. Ion Channel-like Crystallographic Signatures in Modified Guanine–Potassium/Sodium Interactions. *Cryst. Growth Des.* **2013**, *13*, 455–459.

(23) Vakiti, R. K.; Garabato, B. D.; Schieber, N. P.; Rucks, M. J.; Cao, Y.; Webb, C.; Maddox, J. B.; Celestian, A.; Pan, W.-P.; Yan, B. Synthesis and Characterization of Two- and Three-Dimensional Calcium Coordination Polymers Built with Benzene-1,3,5-tricarboxylate and/or Pyrazine-2-carboxylate. *Cryst. Growth Des.* **2012**, *12*, 3937–3943.

(24) Wang, J.-P.; Lu, Z.-J.; Zhu, Q.-Y.; Zhang, Y.-P.; Qin, Y.-R.; Bian, G.-Q.; Dai, J. Calcium and Magnesium Bicarboxylates Combined with Tetrathiafulvalene Moiety. *Cryst. Growth Des.* **2010**, *10*, 2090–2095.

(25) Kam, K. C.; Young, K. L. M.; Cheetham, A. K. Chemical and Structural Diversity in Chiral Magnesium Tartrates and their Racemic and Meso Analogues. *Cryst. Growth Des.* **2007**, *7*, 1522–1532.

(26) Reich, H. J. What's Going on with These Lithium Reagents? *J. Org. Chem.* **2012**, *77*, 5471–5491.

(27) Ahrens ionic radii are based on interionic distance measurements of solid state crystal structures. They are used here to give an idea of the relative sizes of the cationic counterions of the metal salts of DMSA. See ref 28 for details on how Ahrens ionic radii were obtained.

(28) Ahrens, L. H. The Use of Ionization Potentials Part 1. Ionic Radii of the Elements. *Geochim. Cosmochim. Acta* **1952**, *2*, 155–169.

(29) Okur, H. I.; Kherb, J.; Cremer, P. S. Cations Bind Only Weakly to Amides in Aqueous Solutions. *J. Am. Chem. Soc.* **2013**, *135*, 5062–5067.

(30) Persson, I. Hydrated Metal Ions in Aqueous Solution: How Regular Are Their Structures? *Pure Appl. Chem.* **2010**, *82*, 1901–1917.

(31) Rummey, J. M.; Boyce, M. C. Introducing the gNMR Program in an Introductory NMR Spectrometry Course to Parallel its Use by Spectroscopist. *J. Chem. Educ.* **2004**, *81*, 762–763.

(32) Roberts, J. D. Fascination with the Conformational Analysis of Succinic acid, as Evaluated by NMR Spectroscopy, and Why. *Acc. Chem. Res.* **2006**, *39*, 889–896.